Article

Discovery Medicine 2024; 36(183): 753–764
https://doi.org/10.24976/Discov.Med.202436183.71

Effect of Calcium Supplementation and TMEM16A Inhibition on Endoplasmic Reticulum Stress Induced by Dental Fluorosis in Mice

Yangyang Yu[1,*,†], Fei Xia[1,†], Rong Liu[1], Yahui Yan[1], Li Yin[2]

[1]Department of Oral Medicine, Huabei Petroleum Administration Bureau General Hospital, 062552 Renqiu, Hebei, China
[2]Department of Internal Medicine, Huabei Petroleum Administration Bureau General Hospital, 062552 Renqiu, Hebei, China
*Correspondence: zyy_yyy2023@163.com (Yangyang Yu)
[†]These authors contributed equally.
Published: 20 April 2024

Background: Dental fluorosis is a discoloration of the teeth caused by the excessive consumption of fluoride. It represents a distinct manifestation of chronic fluorosis in dental tissues, exerting adverse effects on the human body, particularly on teeth. The transmembrane protein 16a (TMEM16A) is expressed at the junction of the endoplasmic reticulum and the plasma membrane. Alterations in its channel activity can disrupt endoplasmic reticulum calcium homeostasis and intracellular calcium ion concentration, thereby inducing endoplasmic reticulum stress (ERS). This study aims to investigate the influence of calcium supplements and TMEM16A on ERS in dental fluorosis.

Methods: C57BL/6 mice exhibiting dental fluorosis were subjected to an eight-week treatment with varying calcium concentrations: low (0.071%), medium (0.79%), and high (6.61%). Various assays, including Hematoxylin and Eosin (HE) staining, immunohistochemistry, real-time fluorescence quantitative polymerase chain reaction (qPCR), and Western blot, were employed to assess the impact of calcium supplements on fluoride content, ameloblast morphology, TMEM16A expression, and endoplasmic reticulum stress-related proteins (calreticulin (CRT), glucose-regulated protein 78 (GRP78), inositol requiring kinase 1α (IRE1α), PKR-like ER kinase (PERK), activating transcription factor 6 (ATF6)) in the incisors of mice affected by dental fluorosis. Furthermore, mice with dental fluorosis were treated with the TMEM16A inhibitor T16Ainh-A01 along with a medium-dose calcium to investigate the influence of TMEM16A on fluoride content, ameloblast morphology, and endoplasmic reticulum stress-related proteins in the context of mouse incisor fluorosis.

Results: In comparison to the model mice, the fluoride content in incisors significantly decreased following calcium supplements ($p < 0.01$). Moreover, the expression of TMEM16A, CRT, GRP78, IRE1α, PERK, and ATF6 were also exhibited a substantial reduction ($p < 0.01$), with the most pronounced effect observed in the medium-dose calcium group. Additionally, the fluoride content ($p < 0.05$) and the expression of CRT, GRP78, IRE1α, PERK, and ATF6 ($p < 0.01$) were further diminished following concurrent treatment with the TMEM16A inhibitor T16Ainh-A01 and a medium dose of calcium.

Conclusions: The supplementation of calcium or the inhibition of TMEM16A expression appears to mitigate the detrimental effects of fluorosis by suppressing endoplasmic reticulum stress. These findings hold implications for identifying potential therapeutic targets in addressing dental fluorosis.

Keywords: dental fluorosis; endoplasmic reticulum stress; TMEM16A; T16Ainh-A01

Introduction

Dental fluorosis represents a form of discolored teeth and serves as an early indicator of chronic fluorosis within the oral cavity. It is marked by the diminished enamel gloss in permanent teeth, often exhibiting a chalky or brownish-yellow appearance, and irregular enamel defects become apparent in severe instances [1]. The impact of dental fluorosis extends significantly to the structure, morphology, and functionality of the teeth. It affects chewing function, digestion, aesthetics, and even the mental health of affected individuals [2].

The onset of dental fluorosis is linked to prolonged and excessive fluoride consumption during the developmental phase of teeth. In the mineralization process of teeth, the enameloblasts within the enamel matrix can undergo damage due to elevated fluoride levels in the body, resulting in impaired enamel development [3,4]. Additionally, fluoride ions contribute to the excessive mineralization of crystals, leading to a reduction in the surrounding concentration of calcium ions [5]. Research indicates that animals with elevated fluoride intake, when supplemented with calcium, experience a significant reduction in fluoride content in the bones, thereby preventing the onset of dental lesions [6].

The mechanism behind the formation of dental fluorosis is intricate, and multiple studies have identified endoplasmic reticulum stress (ERS) induced by ameloblasts following excessive fluoride intake as a key factor in the development of dental fluorosis [7,8].

The endoplasmic reticulum (ER) functions as a crucial site for protein processing and folding within the cellular environment [9]. To ensure the optimal folding of proteins, the ER environment must be maintained in equilibrium. When this balance is disturbed, ERS occurs [10], and in severe cases, it can lead to cell apoptosis [11]. In response to stress conditions, ER dysfunction may result in the accumulation of unfolded or misfolded proteins, triggering the unfolded protein response (UPR). The UPR is designed to eliminate these abnormal proteins through degradation or autophagy, thereby preserving cellular homeostasis [12]. Fluorine has the ability to inhibit protein synthesis, alter the spatial morphology of proteins, and promote ERS [13]. In a study by Zhang *et al*. [9], the mouse ameloblastoid cell line LS8 was treated with varying concentrations of NaF. The molecular chaperones associated with ERS, including calreticulin (CRT), glucose-regulated protein 78 (GRP78), Xbox-binding protein 1 (XBP1), and Caspase-12, exhibited up-regulation, indicating that fluoride has the potential to induce ERS in enameloblasts, subsequently contributing to the development of dental fluorosis [14].

The regulation of calcium homeostasis plays a crucial role in dental fluorosis development. Studies have demonstrated that NaF can rapidly open the membrane Ca^{2+} channel within a short time frame (20 s), leading to a swift increase in the concentration of Ca^{2+} in human osteoblasts [15]. Abnormally elevated intracellular Ca^{2+} concentrations disrupt the calcium balance of ER, leading to ERS and subsequent apoptosis [16].

Glucose-regulated protein 78 (GRP78) is a vital molecular chaperone integral to the process of ERS. GRP78 forms a dimer with receptors, including inositol requiring enzyme 1 (IRE1), PKR-like ER kinase (PERK), and activating transcription factor 6 (ATF6) [17]. In the event of ERS, GRP78 dissociates from the transmembrane receptor, initiating the binding of unfolded proteins and triggering the UPR. This response aims to mitigate the accumulation of unfolded or misfolded proteins, ultimately restoring the normal function of the ER [18].

CRT serves as another molecular chaperone associated with ERS, localized in the ER. Its role involves the regulation of the accumulation and release of Ca^{2+}, contributing to the maintenance of intracellular calcium homeostasis [19]. Recognized as Anoctamin-1, transmembrane protein 16 (TMEM16) belongs to the TMEM protein family, a category of membrane proteins. It functions as a gene encoding a calcium-activated chloride channel. TMEM16A is widely expressed in various cells and plays a significant role in processes such as light conduction, olfactory development, smooth muscle contraction, nociceptive sensation, and cell proliferation [20]. Dysfunction of TMEM16A has been associated with diseases including cancer, asthma, gastrointestinal movement disorders such as diarrhea, and pulmonary cystic fibrosis [21].

Recent reports suggest that the expression of TMEM16A expression at the ER-plasma junction is affected by calcium release mediated through inositol 1,4,5-trisphosphate (IP3) receptors. Limited investigations have documented the involvement of TMEM16A's in the modulation of ERS within dental fluorosis mice.

The objective of this study was to develop a mouse model of dental fluorosis and evaluate the effects of different Ca^{2+} concentrations on the expression of TMEM16A and proteins related to endoplasmic reticulum stress (ERS). The study also delved into understanding the impact of inhibiting TMEM16A expression on the levels of ERS-related proteins. This investigation aims to offer fresh insights into the mechanisms underlying the pathogenesis of dental fluorosis and potential interventions for its treatment.

Materials and Methods

Materials

C57BL/6 mice were obtained from Chongqing Ensiweier Biotechnology Co., Ltd. (Chongqing, China). T16Ainh-A01 (S28110) was purchased from Shanghai Yuanye Bio-Technology Co., Ltd. (Shanghai, China). A 3% solution of pentobarbital sodium (P3761) was acquired from Beijing BSZH Scientific Company (Beijing, China). The colorimetric assay kit for calcium (S1063S) was sourced from Beyotime Biotechnology (Beijing, China). The fluorosis determination reagent kit (8308151) was obtained from Lohand Biological Company (Hangzhou, China). Essential materials, including phosphate-buffered saline (PBS) (G0002), hematoxylin staining (G1004), eosin staining (G1002), protease K (G1234), Sodium dodecyl sulfate-polyacrylamide gel electrophoresis (SDS-PAGE) Running Buffer (G2018), were supplied by Wuhan Servicebio Technology Co., Ltd. (Wuhan, China). A 10% solution of ethylenediamine tetraacetic acid (EDTA) decalcification solution (DD0002) was procured from Beijing Leagene Biotechnology Co., Ltd. (Beijing, China). Additionally, goat serum (C0265), Radio Immunoprecipitation Assay (RIPA) lysis buffer (P0013B), and Bicinchoninic acid (BCA) detection kit (P0010) were purchased from Shanghai Beyotime Biotechnology (Shanghai, China).

Primary antibodies CRT (bs-5913R) and TMEM16A (bs-3794R) were procured from Beijing Bioss Technology Co., Ltd. (Beijing, China). Goat Anti-Rabbit IgG H&L (HRP) (511203) was obtained from Chengdu Zen-Bioscience Co., Ltd. (Chengdu, China). Diaminobenzidine (DAB) color solution (ZLI-9019) was sourced from Beijing Zhongshan Goldenbridge Biotechnology Co., Ltd. (Beijing, China). Trizol, chloroform, ethanol, and xylene were purchased from Chongqing Chuandong Chemical (Group)

Co., Ltd. (Chongqing, China). The Goldenstar™ RT6 cDNA Synthesis Kit Ver.2 (TSK302M) and 2 × T5 Fast real-time fluorescence quantitative polymerase chain reaction (qPCR) Mix (SYBR Green I) (TSE002) were acquired from Beijing Tsingke Biotechnology Co., Ltd. (Beijing, China). The BCA Assay Kit Protein Loading Buffer (8015011) was purchased from Dakewe Biotech Co., Ltd. (Shenzhen, China). Antibodies TMEM16A (A10498), GRP78 (A0241), IRE1α (A17940), PERK (A21255), ATF6 (A0202), and glyceraldehyde 3-phosphate dehydrogenase (GAPDH) (A19056) were sourced from Wuhan ABclonal Biotechnology Co., Ltd. (Wuhan, China). Polyvinylidene fluoride (PVDF) membrane (10600023) was purchased from Amersham (Freiburg, Germany). Phenylmethanesulfonyl fluoride (PMSF) (P408676) was obtained from Aladdin biochemical technology (Shanghai, China). Enhanced Chemiluminescence (ECL) exposure solution (34580) was purchased from Thermo (Waltham, MA, USA).

Methods

Animal Grouping and Model Construction

A total of 48 female C57BL/6 mice, aged 1 month, were subjected to a uniform feeding regimen for 7 days. The animal facility maintained a temperature of 23 ± 2 °C, with humidity ranging between 35–60%, and operated on a 12-hour light/dark cycle. Subsequently, the mice were randomly allocated into six groups: blank control, model, low calcium, medium calcium, high calcium, and medium calcium + TMEM16A inhibitor T16Ainh-A01 (50 mg/kg/d) group, each comprising 8 mice. These groups were established to assess the impact of various calcium-containing feed treatments on fluoride content, TMEM16A expression, and ERS-related proteins in the incisors of mice with dental fluorosis. Each group received drinking water containing 100 mg/L NaF, and the calcium content in the calcium feed varied as low (0.071%), medium (0.79%), and high (6.61%). Following 8 weeks of breeding, the mice were anesthetized with 3% pentobarbital sodium and then subsequently euthanized by decapitation. The jaws with incisors were separated and the incisor specimens were collected for further analysis.

Determination of Fluoride and Calcium Content

The mice were subjected to weekly observations to assess their overall status and incisor fluorosis morphology. The focus of incisor fluorosis observation in each group included monitoring changes in color, gloss, the presence of streaks and dents, excessive abrasion, rupture, irregular arrangement of incisors, and the presence of defects. Subsequent to incisor grinding, both calcium and fluorosis content in the incisors were determined utilizing the colorimetric assay kit for calcium and the fluorosis determination reagent kit. Fluoride absorbance was measured at a wavelength of 313.3 nm using an atomic absorption spectrophotometer (240FS AA, Agilent, Tokyo, Japan), while calcium absorbance was measured at 422.7 nm.

Hematoxylin and Eosin (HE) Staining

The incisor specimen underwent a thorough procedure: rinsing with PBS, fixation in a 4% paraformaldehyde solution, decalcification with a decalcifying agent, cleaning, and sequential immersion in 70% ethanol for 6 hours, 80% ethanol for 2 hours, 90% ethanol for 4 hours, 100% ethanol I for 1 hour, 100% ethanol II for 1 hour, and 100% ethanol III for 2 hours. Subsequently, the specimens were immersed in xylene I and xylene II for 45 minutes each, embedded in molten paraffin, allowed to solidify, and then sectioned into slices of 2.5 µm thickness.

These sections were laid flat on slip-resistant slides, placed in a baking machine at 55 ℃ to ensure firm adherence of tissue sections to the slide. After dewaxing and rehydration, the sections underwent a triple rinse with distilled water before undergoing hematoxylin and eosin staining. Image acquisition was performed using a microscope model Mshot MF53 (Guangzhou Micro-shot Technology Co., Ltd., Guangzhou, China).

Immunohistochemistry (IHC)

After dewaxing and rehydration, the sections underwent three washes with distilled water and were then treated with a Protease K-induced antigen repair solution for 20 minutes to enhance the detectability of the target antigen in tissue sections. Following a 15 minute exposure to 3% hydrogen peroxide at room temperature, the slides were blocked with goat serum for 60 minutes at room temperature to minimize non-specific binding.

An antibody targeting calreticulin (CRT) or transmembrane protein 16 (TMEM16) (dilution ratio 1:200) was introduced for overnight incubation at 4 °C. Subsequently, Goat Anti-Rabbit IgG H&L (HRP) (dilution ratio 1:500) was applied and incubated at room temperature for 1.5 hours. The DAB color development solution was added for a 1 minute incubation away from light, followed by a 5 minute rinse with tap water. The slices underwent a 1 minute hematoxylin staining, treated with a 1% ethanol hydrochloride solution for 2 seconds, and rinsed with tap water for 10 minutes. Following two cycles of 95% ethanol dehydration for 2 minutes each, the samples underwent a 2 minute dehydration process. Images were captured using a microscope subsequent to the sealing process.

qPCR

Total RNA extraction was carried out using the Trizol method [22]. The Goldenstar™ RT6 cDNA Synthesis Kit Ver.2 was utilized for cDNA synthesis. In a microcentrifuge tube without nuclease, 1 µL gDNA remover, 1 µL 10 × gDNA remover Buffer, and Total RNA (1000 ng) were combined. RNase Free dH_2O was then added to achieve

a final volume of 10 µL. The mixture was incubated for 2 minutes at 42 °C, followed by 5 minutes at 60 °C, and then placed on ice for rapid cooling. After a brief centrifugation, the mixture was supplemented with 4 µL 5 × Goldenstar™ Buffer, 1 µL Goldenstar™ Oligo (dT) 17/Randomer/U6-F, 1 µL DTT, and 1 µL Goldenstar™ RT6. Additionally, 1 µL dNTP Mix was added, and RNase Free dH_2O was introduced to reach a total volume of 20 µL. The reaction parameters were set as follows: 25 °C for 10 minutes, 55 °C for 30 minutes, 85 °C for 5 minutes, and then maintained at 4 °C.

The PCR reaction solution was prepared on ice, comprising 10 µL 2 × T5 Fast qPCR Mix (SYBR Green I), 0.8 µL Primer F, 0.8 µL Primer R, and 1 µL Template cDNA. ddH_2O was added to achieve a final volume of 20 µL. The thermal cycling protocol commenced with an initial denaturation step at 95 °C for 30 seconds, followed by 40 cycles consisting of 5 seconds at 95 °C and 30 seconds at 60 °C. Glyceraldehyde 3-phosphate dehydrogenase (GAPDH) served as an internal reference gene for normalization, and the calculation of relative gene expression was carried out using the $2^{-\Delta\Delta Ct}$ method. Table 1 presents the specific primers employed in the qPCR analysis.

Table 1. Primer sequences.

Primer names	Sequences
TMEM16A-F	TTGATAACCCTGCCACCGTC
TMEM16A-R	CCTGTGAGGTCCCATCGGTA
GRP78-F	ATCGACTTGGGGACCACCTA
GRP78-R	AGTGAAGGCCACATACGACG
IRE1α-F	ATGCCTCTCCCTCAATGGTG
IRE1α-R	TGTTTGGGCAGGTTGTTAGG
PERK-F	GCAGCGGAAGGAGTCTGAA
PERK-R	AAAGACAACGCCAAAGCCAC
ATF6-F	TTCTGGGAGTGAGCTGCAAG
ATF6-R	GGGAACCGAGGAGCTTTTGA
GAPDH-F	TGGTGAAGCAGGCATCTGAG
GAPDH-R	TGAAGTCGCAGGAGACAACC

TMEM16A, transmembrane protein 16a; GRP78, glucose-regulated protein 78; IRE1α, inositol requiring kinase 1α; PERK, PKR-like ER kinase; ATF6, activating transcription factor 6; GAPDH, glyceraldehyde 3-phosphate dehydrogenase.

Western Blot

Following incisor grinding, the obtained powder was transferred into a pre-cooled 1.5 mL centrifuge tube. The specimens were treated with RIPA lysis buffer supplemented with protease and phosphatase inhibitors, along with phenylmethanesulfonyl fluoride (PMSF) to inhibit and block the activity of proteases and phosphatases, ensuring the integrity and stability of the target protein. The mixture was then vortexed for 1 minute and left on ice for 10 minutes until complete lysis. The tissue homogenate in the mortar was transferred to a new 1.5 mL centrifuge tube and centrifuged. The resulting supernatant was collected and stored at –80 °C. The total protein concentration was determined using the BCA method. A total of 500 µg of total protein was combined with 5 × SDS loading buffer in a ratio of 4:1. The protein was denatured by exposure to heated water at 100 °C for 6 minutes.

Denatured proteins were separated by SDS-PAGE gel electrophoresis, with each well loaded with 20 µg of proteins. The proteins were subsequently transferred to a PVDF membrane and blocked with a blocking buffer containing 5% skim milk at 25 °C for 1 hour to prevent nonspecific binding. After an overnight incubation at 4 °C with primary antibodies against TMEM16, GRP78, IRE1α, PERK, ATF6, and GAPDH (dilution ratio 1:1000), Goat Anti-Rabbit IgG H&L (HRP) was applied. This was followed by incubation at 25 °C for 1 hour, with a dilution ratio of 1:2000.

Finally, the entire membrane was evenly covered with a mixture of A and B solutions of ECL exposure solution, and the reaction was detected by exposing it to a Universal Hood II exposure instrument (Bio-Rad) (HOOD-II, Hercules, CA, USA) for 1 minute. ImageJ software was employed for quantifying the signal intensity of the target protein (version 1.48 b, National Institutes of Health, Bethesda, MD, USA).

Data Analysis

Data analysis was performed using GraphPad Prism version 8 (GraphPad Software Company, San Diego, CA, USA) through one-way analysis of variance (ANOVA) followed by Tukey's post hoc test. The data results were presented as mean ± standard deviation. Each test was repeated a minimum of three times. Statistical significance was considered for p values less than 0.05.

Results

Effect of Calcium Supplements on Calcium and Fluorine Content in Incisor Fluorosis of Mice

Compared to the control group, mice treated with NaF exhibited lower calcium levels and higher fluoride levels in the mouse incisors. After 8 weeks of calcium supplements in incisor fluorosis mice, the calcium content in incisors in the calcium-treated group showed a significant increase, while the fluoride content displayed a marked decrease compared to the model group ($p < 0.01$). Treatment with medium-dose calcium (0.79%) exerted the most significant inhibitory effect on fluoride content (Fig. 1A).

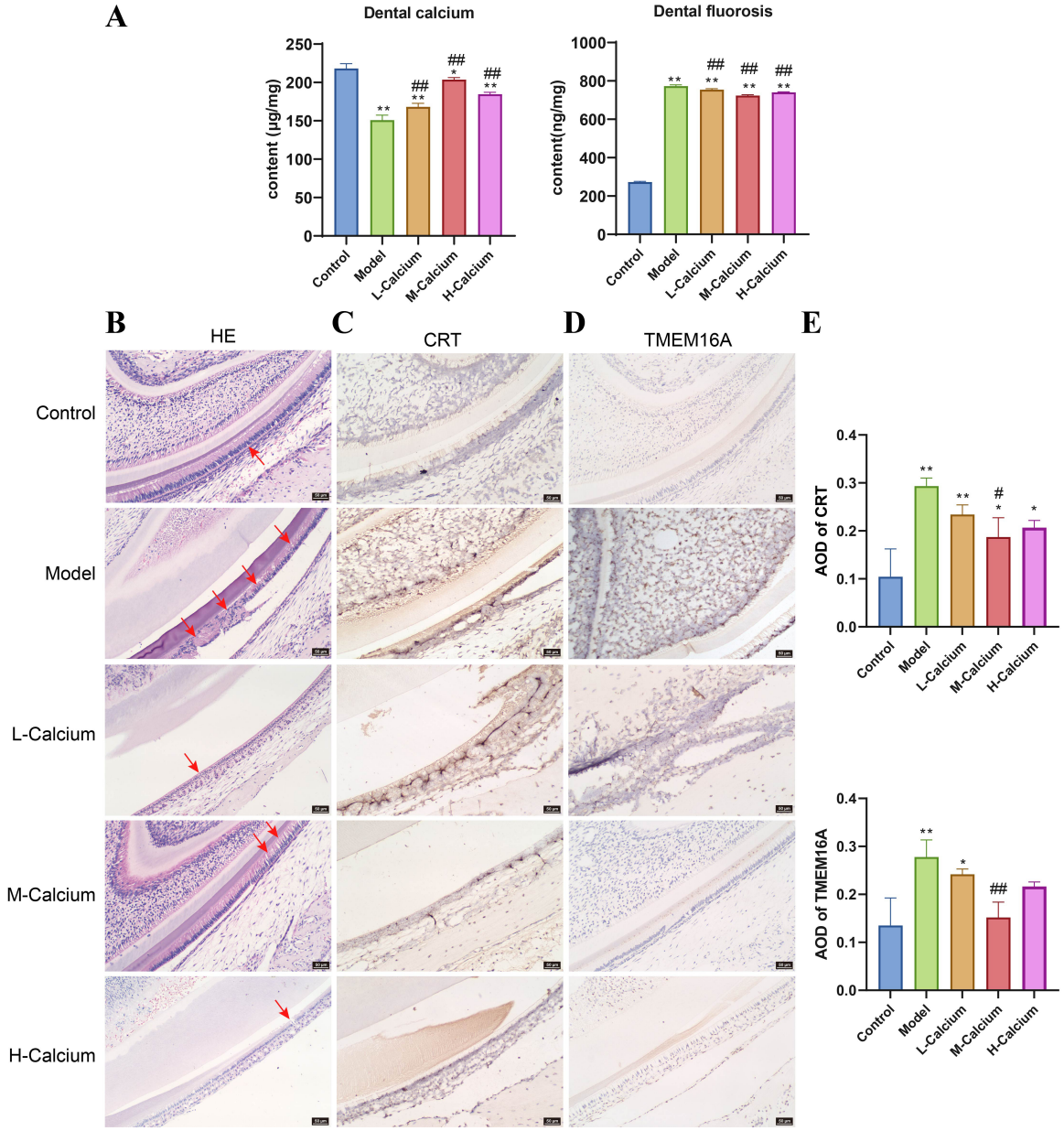

Fig. 1. Investigating the impact of varying calcium supplementation levels on fluorine content, enameloblast morphology, and calreticulin (CRT) and transmembrane protein 16a (TMEM16A) proteins in mice with incisor fluorosis. (A) Effects of calcium treatment on calcium and fluorine content in incisors of mice with incisor fluorosis. (B) Effect of calcium supplements on the morphology and function of enameloblasts in incisors using Hematoxylin and Eosin (HE) staining. The differences of HE results were marked with arrows. Scale bar = 50 μm. (C) Immunohistochemistry detects CRT expression levels within the incisors of mice with dental fluorosis. Scale bar = 50 μm. (D) Immunohistochemistry detects TMEM16A expression levels within the incisors of mice with dental fluorosis. Scale bar = 50 μm. (E) Average Optical Density (AOD) of CRT and TMEM16A protein. *$p < 0.05$, **$p < 0.01$ in comparison to the control group; #$p < 0.05$, ##$p < 0.01$ in comparison to the model group, n = 3. L-Calcium, Group with low calcium intake; M-Calcium, Group with moderate calcium intake; H-Calcium, Group with high calcium intake.

Effect of Calcium Supplements on the TMEM16A Expression and Proteins Associated with ERS in the Incisors of Dental Fluorosis-Afflicted Mice

In the control group, the enameloblasts appeared as tall columnar cells, densely and regularly arranged, with clear nucleoplasmic distinction. In the model group, low-calcium group, and high-calcium group, the height of enameloblasts shortened with distorted morphology, and the change in the model group was the most significant. Most cells exhibited irregular vacuoles. In the medium calcium group, the enameloblasts showed relatively tall columnar cells, tightly and regularly arranged, resembling the mor-

phology of the control group (Fig. 1B). These results suggest that calcium supplementation can restore the columnar morphology and arrangement of enameloblasts, with the best effect observed in the calcium group.

Through IHC, highly expressed TMEM16A and CRT proteins were observed in the model group mice ($p < 0.01$), while they were poorly expressed in the calcium-treated group. TMEM16A and CRT protein expressions exhibited the lowest levels in the medium-calcium group ($p < 0.05$) (Fig. 1C–E).

At the molecular level, TMEM16A, GRP78, IRE1α, PERK, and ATF6 mRNAs and protein expression showed significantly higher levels after NaF treatment than in the control group ($p < 0.01$). TMEM16A, GRP78, IRE1α, PERK, and ATF6 mRNAs and protein expression exhibited a marked reduction in the calcium-treated groups compared to the model group ($p < 0.01$), with the most significant decrease observed in the moderate calcium intake group (Fig. 2A,B). Overall, calcium supplements reduced the expression of TMEM16A, GRP78, IRE1α, PERK, and ATF6 mRNAs and proteins, and the medium-calcium (0.79%) treatment provided the best response to ERS alleviation.

Effect of T16Ainh-A01 on Calcium and Fluorine Content in Incisors of Mice with Dental Fluorosis

The TMEM16A inhibitor T16Ainh-A01 was administered to incisor fluorosis mice with medium-calcium to investigate the impact of TMEM16A on fluorosis. In comparison to mice treated with medium-calcium alone, those treated with T16Ainh-A01 and medium-calcium exhibited significantly higher calcium content but significantly lower fluorine content in incisors ($p < 0.05$) (Fig. 3A).

Impact of T16Ainh-A01 on TMEM16A and ERS Related Proteins Expression in the Incisors of Mice with Dental Fluorosis

In the control group, the enameloblasts appeared as tall columnar cells, densely and regularly arranged, with clear nucleoplasmic distinction. In the model group, enameloblasts were shortened, distorted in morphology, and had irregular vacuoles in most cells. In the medium-calcium group and the medium-calcium + T16Ainh-A01 group, the enameloblasts showed relatively tall columnar morphology, tightly and regularly arranged, with the medium-calcium + T16Ainh-A01 group resembling the morphology of the control group (Fig. 3B). This indicates that both calcium supplementation and inhibition of T16Ainh-A01 contribute to the restoration of enameloblasts morphology.

Highly expressed TMEM16A and CRT proteins were observed in the model group mice ($p < 0.01$), while they were poorly expressed in the medium-calcium treated group ($p < 0.05$), with the lowest expression in the medium-calcium + T16Ainh-A01 group (CRT: $p < 0.05$, TMEM16A: $p > 0.05$) (Fig. 3C–E).

At the molecular level, TMEM16A, GRP78, IRE1α, PERK, and ATF6 mRNAs and protein expression were significantly higher after NaF treatment than in the control group ($p < 0.01$). In contrast to the model group, the expression of TMEM16A, GRP78, IRE1α, PERK, and ATF6 mRNAs and proteins after medium-calcium treatment was significantly reduced ($p < 0.05$), and the medium-calcium + T16Ainh-A01 group had the lowest expression ($p < 0.05$) (Fig. 4A,B). These results suggest that calcium supplementation and inhibition of TMEM16A expression can improve the calcium content and enameloblasts damage in incisors of mice with dental fluorosis, while also alleviating the severity of ERS.

Discussion

Dental fluorosis is a distinct manifestation of chronic fluorosis affecting dental tissues. Excessive fluoride intake can result in diminished enamel mineralization and heightened porosity, leading to developmental disorders in enamel. This condition not only harms the incisors and bones but also poses risks to vital organs such as the endocrine system, neuromuscular system, liver, and kidneys. The detrimental effects extend beyond appearance, emphasizing the importance of addressing fluorosis for overall health. Research indicates that a deficiency in calcium can exacerbate dental fluorosis formation [23], while increased calcium intake has been shown to enhance enamel structure and improve resistance to dental caries [24].

Subsequent investigations have demonstrated that following Ca^{2+} supplementation, Ca^{2+} binds with F^- to form insoluble CaF_2 in the gastrointestinal tract or bloodstream. This process reduces the concentration of free F^- and facilitates the normal progression of enamel mineralization [25,26]. Additionally, research by Yu *et al.* [27] revealed that, in rats subjected to excessive fluoride intake, both blood and bone fluoride levels increased over time in groups treated with low calcium and normal calcium. Conversely, rats treated with high calcium showed minimal changes in blood and bone fluoride levels. Moreover, the severity of dental fluorosis was most pronounced in the low-calcium group and milder in the high-calcium group [27].

Our findings suggest that supplementing an appropriate amount of calcium can mitigate fluoride content in the incisors of fluorosis mice by binding with F^-. Furthermore, it can ameliorate the damage to enameloblasts caused by fluoride toxicity. This implies that an adequate calcium intake may counteract the adverse effects of fluoride on teeth by reducing fluoride accumulation in the body. However, the complete mechanism underlying dental fluorosis remains to be fully elucidated. Existing research suggests that dental fluorosis primarily arises from fluoride's impact on the ER function of enameloblasts, leading to disruptions in protein synthesis [8,28].

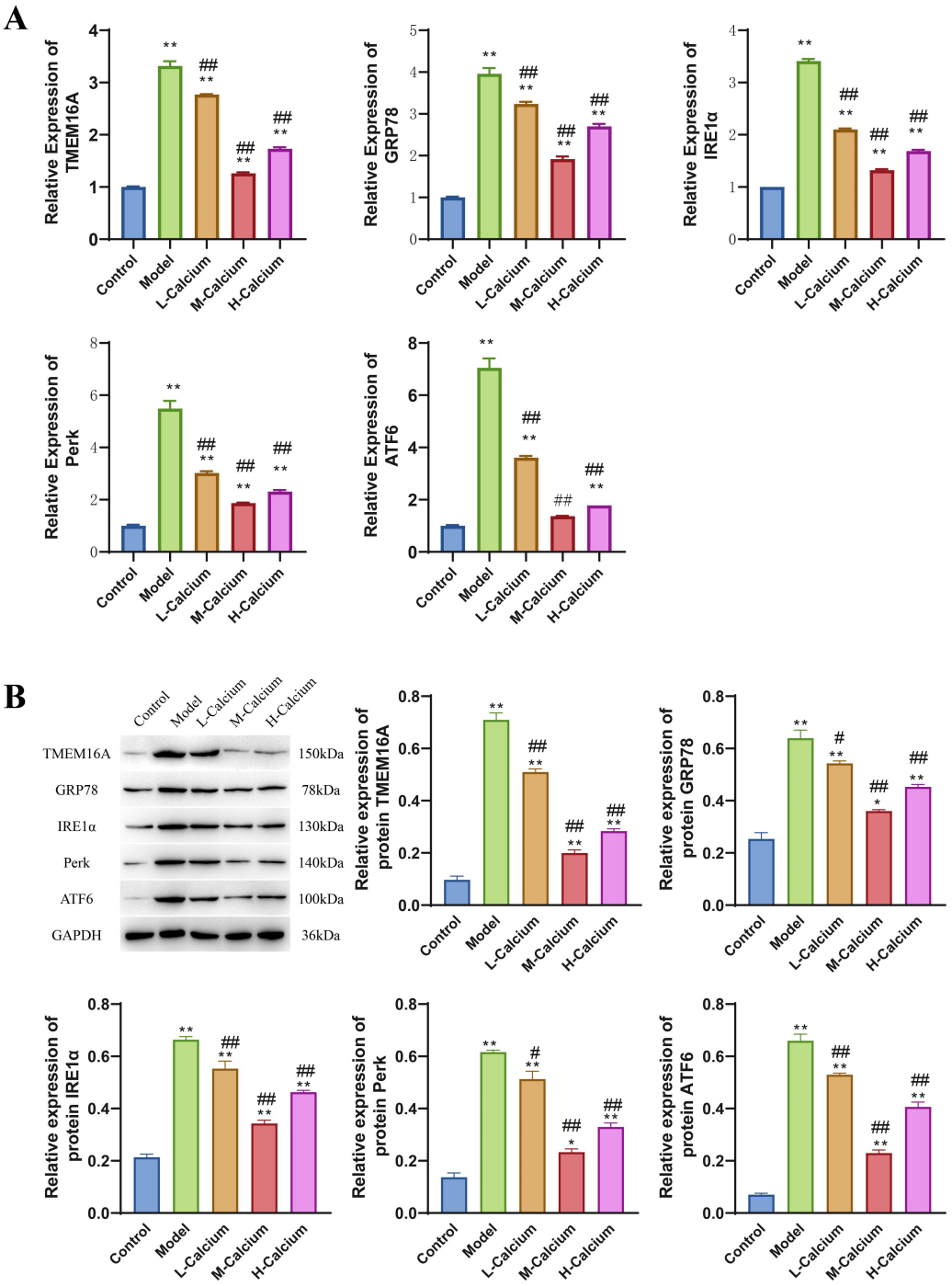

Fig. 2. Effect of calcium supplements on TMEM16A and endoplasmic reticulum stress (ERS) related proteins in mice with dental fluorosis. (A) Real-time fluorescence quantitative polymerase chain reaction (qPCR) detects the expression levels of TMEM16A, glucose-regulated protein 78 (GRP78), inositol requires kinase 1α (IRE1α), PKR-like ER kinase (PERK), and activating transcription factor 6 (ATF6) mRNAs in the mouse incisors. (B) Western blot detects the expression levels of TMEM16A, GRP78, IRE1α, PERK, and ATF6 proteins. *$p < 0.05$, **$p < 0.01$ in comparison to the control group; #$p < 0.05$, ##$p < 0.01$ in comparison to the model group, n = 3. L-Calcium, Group with low calcium intake; M-Calcium, Group with moderate calcium intake; H-Calcium, Group with high calcium intake.

Sharma *et al*. [29] demonstrated that low fluoride levels significantly stimulate ESR in enameloblasts through *in vitro* culture experiments. When ESR occurs, it affects the synthesis and breakdown of amelogenin, leading to an increase in unfolded protein reaction (UPR) proteins but a reduction in minerals in enameloblasts. This results in incom-

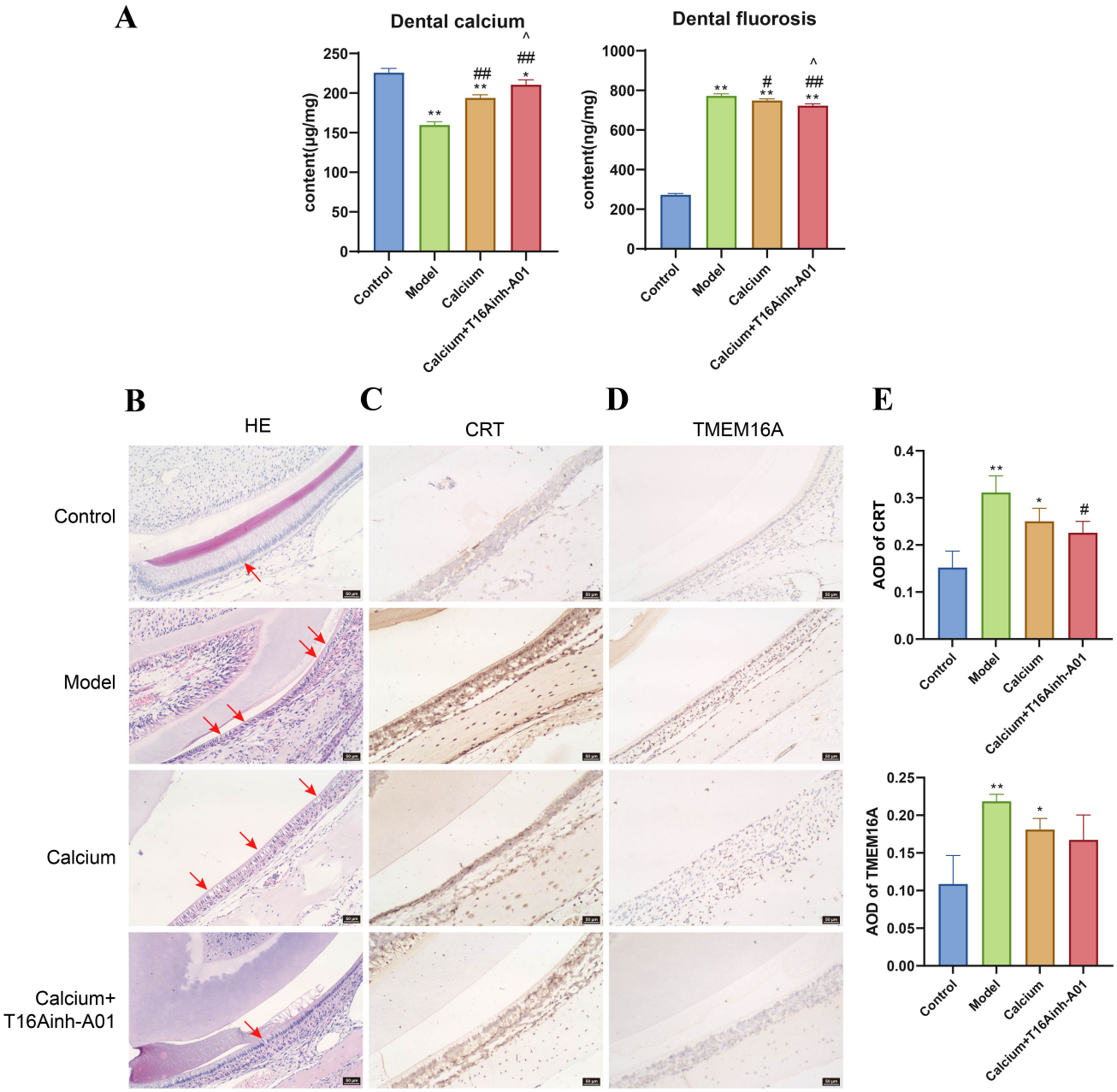

Fig. 3. Effects of T16Ainh-A01 on fluorine content, enameloblast morphology, and CRT and TMEM16A proteins in dental fluorosis mice. (A) Effect of T16Ainh-A01 on calcium and fluorine content in mouse incisor fluorosis. (B) Effect of calcium supplements and T16Ainh-A01 on the morphology and function of enameloblasts using HE staining. The differences of HE results were marked with arrows. Scale bar = 50 μm. (C) Immunohistochemistry detects CRT expression in the incisors of mice with dental fluorosis. Scale bar = 50 μm. (D) Immunohistochemistry detects TMEM16A expression in incisors of fluorosis mice. Scale bar = 50 μm. (E) Average Optical Density (AOD) of CRT and TMEM16A protein. $*p < 0.05$, $**p < 0.01$ in comparison to the control group; $\#p < 0.05$, $\#\#p < 0.01$ in comparison to the model group. $\hat{}p < 0.05$ in comparison to the calcium group, n = 3. Control, Control group; Model, Model group; Calcium, Medium-calcium group; Calcium + T16Ainh-A01, medium calcium + T16Ainh-A01 group.

plete mineralization of the enamel and the formation of incisor fluorosis [14]. The unfolded protein response (UPR) plays a role in restoring ER equilibrium by reducing protein synthesis, enhancing the ER's protein folding capacity, and eliminating unfolded or misfolded proteins [30].

The solution to ERS involves ER transmembrane proteins: inositol requiring enzyme 1α (IRE1α), PKR-like ER kinase (PERK), and activating transcription factor 6 (ATF6), which can regulate various specific and overlapping ERS responses [31]. Glucose-regulated protein 78 (GRP78) serves as a principal ER chaperone, and typically,

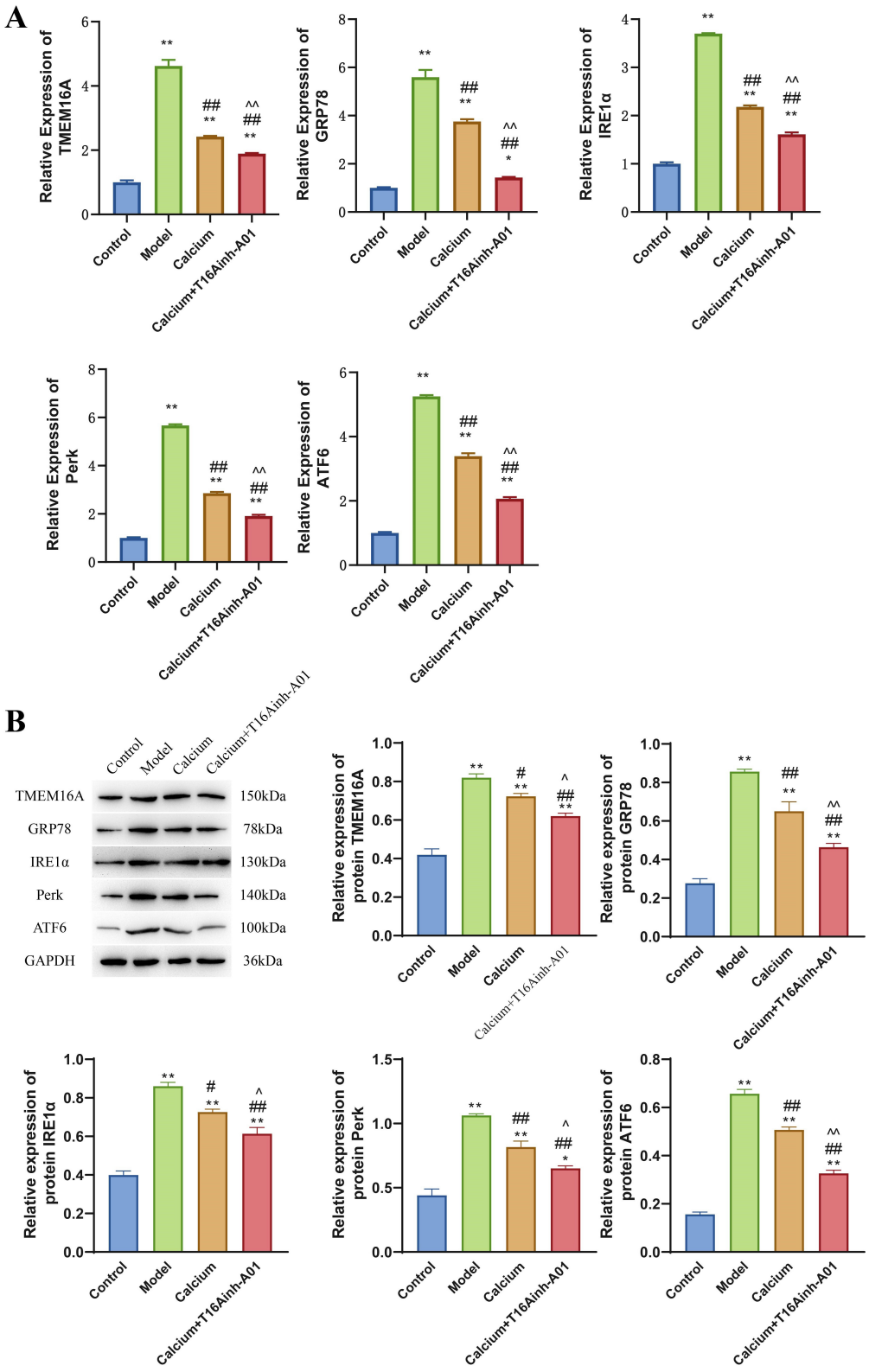

Fig. 4. Impact of T16Ainh-A01 on TMEM16A and ERS-related proteins expression in the incisors of mice with dental fluorosis. (A) qPCR detects the mRNA expression of TMEM16A, GRP78, IRE1α, PERK, and ATF6 in the mouse incisors. (B) Western blot detects the protein expression of TMEM16A, GRP78, IRE1α, PERK, and ATF6 expression. *$p < 0.05$, **$p < 0.01$ in comparison to the control group; #$p < 0.05$, ##$p < 0.01$ in comparison to the model group. ^$p < 0.05$, ^^$p < 0.01$ in comparison to the medium-calcium group, n = 3. Control, Control group; Model, Model group; Calcium, Medium-calcium group; Calcium + T16Ainh-A01, medium calcium + T16Ainh-A01 group.

the mentioned proteins bind to GRP78. When ERS occurs, GRP78 is activated, and the ER transmembrane protein is separated from GRP78 and activated [32]. IRE1α is a widely conserved dual enzyme with both kinase and endonuclease activity. Under ERS conditions, IRE1 dissociates from GRP78, specifically cleaving XBP-1 mRNA. The spliced XBP1 increases the level of the ERS molecular chaperone, facilitating the restoration of cellular homeostasis [33].

PERK belongs to the eIF2α protein kinase family, the UPR initiated by PERK is similar to IRE1. PERK responds to ERS through auto-phosphorylation and homologous multimerization when dissociating from GRP78 or reducing ER membrane mobility [34]. When ERS occurs, ATF is activated and translocated to the Golgi bodies. Golgi protease cleaves its transmembrane fragments, and the cleaved fragments can be transferred to the nucleus to promote the transcription of transcription factors XBP1 and GRP78/BIP and C/EBP Homologous Protein (CHOP), enhancing protein folding function and alleviating ERS [35,36].

Both PERK and IRE1α undergo dimerization and autophosphorylation when GRP78 dissociates or ER membrane mobility decreases [37], leading to increased expression of IRE1 and PERK in cells. In our study, a significant increase in the expression of GRP78, IRE1α, PERK, and ATF in the incisors of fluoride-poisoned mice was observed, indicating that fluoride induces ERS, consistent with the study by Zhang *et al*. [38]. However, after supplementing calcium in appropriate amounts, the expression of these genes decreased, indicating that calcium can alleviate ERS caused by fluoride toxicity.

Effective and rapid folding of glycoproteins in the ER requires the involvement of the molecular chaperone Calreticulin (CRT). CRT is a member of the Calnexin family, and it exists as a soluble protein within the ER, relying on both Ca^{2+} and ATP for its functioning. Research has demonstrated a notable elevation in CRT levels after enameloblasts are treated with NaF. The increased CRT levels and subsequent release of Ca^{2+} could contribute to the disruption of calcium homeostasis in the ER, leading to ERS [39].

Zhang *et al*. [38] discovered that the expression of CRT in the high-fluoride group and low-fluoride group was significantly higher than that in the negative control group, and as the fluoride concentration increased, the intracellular Ca^{2+} concentration in enameloblasts also increased. When the Ca^{2+} exceeds the regulatory range of enameloblasts, it promotes the cells to enter an ERS state, leading to protein synthesis disorders [38]. TMEM16A (Anoctamin-1) is a calcium-activated chloride channel that becomes operational upon intracellular Ca^{2+} activation [40], and it plays a key physiological function in ion transport and the regulation of other ion channels. Studies have shown that overexpression of TMEM16A can cause breast cancer ERS through the initiation of the PERK and IRE1 pathways within the UPR [41]. Additionally, overexpression of TMEM16A may lead to abnormal calcium ion metabolism, disrupting the differentiation and mineralization of enameloblasts [42]. However, the specific role of TMEM16A in ERS due to fluoride toxicity is not yet fully understood.

The results of our study indicate that supplementing an appropriate amount of calcium can reduce the fluoride content in the incisors of fluorosis mice, inhibit the expression of TMEM16A and CRT, which is consistent with the findings of Zhang *et al*. [38]. Furthermore, inhibiting TMEM16A was found to further reduce fluoride content, improve enameloblast damage caused by fluoride toxicity, and suppress the expression of CRT, GRP78, IRE1α, PERK, and ATF6. This suggests that TMEM16A may play a role in alleviating fluoride-induced enameloblast ERS by affecting Ca^{2+} metabolism and the GRP78, IRE1α, PERK, and ATF6 pathways.

These findings provide a new perspective for identifying potential therapeutic targets for dental fluorosis. However, further research is needed to fully understand the specific mechanism by which TMEM16A activates enameloblast ERS in dental fluorosis. Continued exploration in this area could contribute to developing more targeted and effective interventions for dental fluorosis.

Conclusions

In summary, the administration of calcium supplements or the suppression of TMEM16A expression may result in a reduction in the expression of ERS-related proteins in dental fluorosis. This suggests a potential correlation between excessive fluorine-induced ERS and TMEM16A. However, the molecular mechanism of action remains unclear, and additional research is necessary in the future. Clinical trials should also be undertaken within the population affected by dental fluorosis to assess the effectiveness and safety of calcium supplements and the inhibition of TMEM16A as potential treatment options.

Availability of Data and Materials

The datasets utilized in the present study can be made available by contacting the corresponding author upon a reasonable request.

Author Contributions

YYY and FX designed the research study, performed the research, and drafted the manuscript. RL mainly contributed to data acquisition and analysis. YHY and LY provided help and advice on the Hematoxylin and Eosin (HE) staining experiments. All authors contributed to editorial changes in the manuscript. All authors read and approved the final manuscript. All authors have participated sufficiently in the work and agreed to be accountable for all aspects of the work.

Ethics Approval and Consent to Participate

This study was carried out with the authorization of Ethics Committee of Huabei Petroleum Administration Bureau General Hospital (Ethical approval No. 2020-06).

Acknowledgment

Not applicable.

Funding

This work was supported by the Health Commission of Hebei Province and the research on the correlation between calcium activated chloride ion channels and the mechanism of dental fluorosis (20210664).

Conflict of Interest

The authors declare no conflict of interest.

References

[1] Wen C, Zhang Q, Xie F, Jiang J. Brick tea consumption and its relationship with fluorosis in Tibetan areas. Frontiers in Nutrition. 2022; 9: 1030344.

[2] Gong QM, Ling JQ, Wei X. Research progress in the pathogenesis mechanism of dental fluorosis. Zhonghua Kou Qiang Yi Xue Za Zhi = Zhonghua Kouqiang Yixue Zazhi = Chinese Journal of Stomatology. 2023; 58: 217–223. (In Chinese)

[3] Cheng X, Chen Q, Sun P. Natural phytochemicals that affect autophagy in the treatment of oral diseases and infections: A review. Frontiers in Pharmacology. 2022; 13: 970596.

[4] Burt BA, Keels MA, Heller KE. The effects of a break in water fluoridation on the development of dental caries and fluorosis. Journal of Dental Research. 2000; 79: 761–769.

[5] Li M, Komasa S, Hontsu S, Hashimoto Y, Okazaki J. Structural Characterization and Osseointegrative Properties of Pulsed Laser-Deposited Fluorinated Hydroxyapatite Films on Nano-Zirconia for Implant Applications. International Journal of Molecular Sciences. 2022; 23: 2416.

[6] Ouyang W, Li Y, Liu Z. Effect caused by uptake of different levels of calcium to enamel fluorosis in rats. Zhonghua Kou Qiang Yi Xue Za Zhi = Zhonghua Kouqiang Yixue Zazhi = Chinese Journal of Stomatology. 2000; 35: 47–49. (In Chinese)

[7] Deng H, Ikeda A, Cui H, Bartlett JD, Suzuki M. MDM2-Mediated p21 Proteasomal Degradation Promotes Fluoride Toxicity in Ameloblasts. Cells. 2019; 8: 436.

[8] Robinson C, Brookes SJ, Bonass WA, Shore RC, Kirkham J. Enamel maturation. Ciba Foundation Symposium. 1997; 205: 156–170; discussion 170–174.

[9] Zhang Y, Zhang K, Ma L, Gu H, Li J, Lei S. Fluoride induced endoplasmic reticulum stress and calcium overload in ameloblasts. Archives of Oral Biology. 2016; 69: 95–101.

[10] Sun S, Duan Z, Wang X, Chu C, Yang C, Chen F, *et al*. Neutrophil extracellular traps impair intestinal barrier functions in sepsis by regulating TLR9-mediated endoplasmic reticulum stress pathway. Cell Death & Disease. 2021; 12: 606.

[11] Schröder M. Endoplasmic reticulum stress responses. Cellular and Molecular Life Sciences: CMLS. 2008; 65: 862–894.

[12] Misaka T, Murakawa T, Nishida K, Omori Y, Taneike M, Omiya S, *et al*. FKBP8 protects the heart from hemodynamic stress by preventing the accumulation of misfolded proteins and endoplasmic reticulum-associated apoptosis in mice. Journal of Molecular and Cellular Cardiology. 2018; 114: 93–104.

[13] Kubota K, Lee DH, Tsuchiya M, Young CS, Everett ET, Martinez-Mier EA, *et al*. Fluoride induces endoplasmic reticulum stress in ameloblasts responsible for dental enamel formation. The Journal of Biological Chemistry. 2005; 280: 23194–23202.

[14] Gao XX, Wang FZ. Progress in the study of risk factors for dental fluorosis. Systemic Medicine. 2017; 2: 152–153, 156. (In Chinese)

[15] Barry EL. Expression of mRNAs for the alpha 1 subunit of voltage-gated calcium channels in human osteoblast-like cell lines and in normal human osteoblasts. Calcified Tissue International. 2000; 66: 145–150.

[16] Lobine D, Sadeer N, Jugreet S, Suroowan S, Keenoo BS, Imran M, *et al*. Potential of Medicinal Plants as Neuroprotective and Therapeutic Properties Against Amyloid-β-Related Toxicity, and Glutamate-Induced Excitotoxicity in Human Neural Cells. Current Neuropharmacology. 2021; 19: 1416–1441.

[17] Marrocco V, Tran T, Zhu S, Choi SH, Gamo AM, Li S, *et al*. A small molecule UPR modulator for diabetes identified by high throughput screening. Acta Pharmaceutica Sinica. B. 2021; 11: 3983–3993.

[18] Wang D, Qiu Y, Fan J, Liu Y, Chen W, Li Z, *et al*. Upregulation of C/EBP Homologous Protein induced by ER Stress Mediates Epithelial to Myofibroblast Transformation in ADTKD-UMOD. International Journal of Medical Sciences. 2022; 19: 364–376.

[19] Arnaudeau S, Frieden M, Nakamura K, Castelbou C, Michalak M, Demaurex N. Calreticulin differentially modulates calcium uptake and release in the endoplasmic reticulum and mitochondria. The Journal of Biological Chemistry. 2002; 277: 46696–46705.

[20] Picollo A, Malvezzi M, Accardi A. TMEM16 proteins: unknown structure and confusing functions. Journal of Molecular Biology. 2015; 427: 94–105.

[21] Bai W, Liu M, Xiao Q. The diverse roles of TMEM16A Ca^{2+}-activated Cl^{-} channels in inflammation. Journal of Advanced Research. 2021; 33: 53–68.

[22] Wang M, Dai M, Wu YS, Yi Z, Li Y, Ren G. Immunoglobulin superfamily member 10 is a novel prognostic biomarker for breast cancer. PeerJ. 2020; 8: e10128.

[23] Su Y, Li YJ, Wan L, Ge LH. Effects of different calcium intake on enamel structure and caries susceptibility in rats. Beijing Journal of Stomatology. 2009; 17: 259–261. (In Chinese)

[24] Adegboye ARA, Christensen LB, Holm-Pedersen P, Avlund K, Boucher BJ, Heitmann BL. Intake of dairy products in relation to periodontitis in older Danish adults. Nutrients. 2012; 4: 1219–1229.

[25] Aoba T, Moreno EC, Tanabe T, Fukae M. Effects of fluoride on matrix proteins and their properties in rat secretory enamel. Journal of Dental Research. 1990; 69: 1248–1255.

[26] Tay N, Gan H, de Sousa FB, Shen L, Nóbrega DF, Peng C, *et al*. Improved mineralization of dental enamel by electrokinetic delivery of F^{-} and Ca^{2+} ions. Scientific Reports. 2023; 13: 516.

[27] Yu J, Jun D, Wang W, Xu C, Wu Y, Shi Y, *et al*. Changes of serum parathyroid hormone in rats with fluorosis under different calcium nutrition conditions. Chinese Journal of Endemic Diseases. 2006; 25: 4. (In Chinese)

[28] Wei W, Gao Y, Wang C, Zhao L, Sun D. Excessive fluoride induces endoplasmic reticulum stress and interferes enamel proteinases secretion. Environmental Toxicology. 2013; 28: 332–341.

[29] Sharma R, Tsuchiya M, Bartlett JD. Fluoride induces endoplasmic reticulum stress and inhibits protein synthesis and secretion. Environmental Health Perspectives. 2008; 116: 1142–1146.

[30] Dušková L, Nohelová L, Loja T, Fialová J, Zapletalová P,

Réblová K, *et al*. Low Density Lipoprotein Receptor Variants in the Beta-Propeller Subdomain and Their Functional Impact. Frontiers in Genetics. 2020; 11: 691.

[31] Podinić T, Werstuck G, Raha S. The Implications of Cannabinoid-Induced Metabolic Dysregulation for Cellular Differentiation and Growth. International Journal of Molecular Sciences. 2023; 24: 11003.

[32] Wang S, Zeng F, Ma Y, Yu J, Xiang C, Feng X, *et al*. Strontium Attenuates Hippocampal Damage via Suppressing Neuroinflammation in High-Fat Diet-Induced NAFLD Mice. International Journal of Molecular Sciences. 2023; 24: 10248.

[33] Wei W, Wang Q, Pang S, Tan S, Sun J, Li M, *et al*. Excessive fluoride exposure induces thymocyte apoptosis and impairs cell division: Roles of the PERK and IRE1 pathways. Toxicology Letters. 2020; 328: 35–44.

[34] Lupachyk S, Watcho P, Stavniichuk R, Shevalye H, Obrosova IG. Endoplasmic reticulum stress plays a key role in the pathogenesis of diabetic peripheral neuropathy. Diabetes. 2013; 62: 944–952.

[35] Duwi Fanata WI, Lee SY, Lee KO. The unfolded protein response in plants: a fundamental adaptive cellular response to internal and external stresses. Journal of Proteomics. 2013; 93: 356–368.

[36] Schindler AJ, Schekman R. In vitro reconstitution of ER-stress induced ATF6 transport in COPII vesicles. Proceedings of the National Academy of Sciences of the United States of America. 2009; 106: 17775–17780.

[37] Yu Y, Yang A, Yu G, Wang H. Endoplasmic Reticulum Stress in Chronic Obstructive Pulmonary Disease: Mechanisms and Future Perspectives. Biomolecules. 2022; 12: 1637.

[38] Zhang KQ, Zhang Y, Liu L, Gu HF, Ma L. Effect of fluoride on the expression of endoplasmic reticulum chaperone in ameloblast of rat incisor. Shanghai Kou Qiang Yi Xue = Shanghai Journal of Stomatology. 2013; 22: 481–486. (In Chinese)

[39] Massaeli H, Viswanathan D, Pillai DG, Mesaeli N. Endoplasmic reticulum stress enhances endocytosis in calreticulin deficient cells. Biochimica et Biophysica Acta. Molecular Cell Research. 2019; 1866: 727–736.

[40] Wang H, Zou L, Ma K, Yu J, Wu H, Wei M, *et al*. Cell-specific mechanisms of TMEM16A Ca^{2+}-activated chloride channel in cancer. Molecular Cancer. 2017; 16: 152.

[41] Zheng YQ. TMEM16A promotes the proliferation of breast cancer cells by regulating the PERK signaling pathway of endoplasmic reticulum stress [master's thesis]. China Medical University. 2022.

[42] Ji W, Shi D, Shi S, Yang X, Chen Y, An H, *et al*. TMEM16A Protein: Calcium-Binding Site and its Activation Mechanism. Protein and Peptide Letters. 2021; 28: 1338–1348.